Supplementary Information

Adsorptive removal of norfloxacin from aqueous solutions by Fe/Cu CNS-Embedded Alginate-Carboxymethyl Cellulose-Chitosan Beads

Geetha Gopal, Amitava Mukherjee*

Centre for Nanobiotechnology, VIT, Vellore, Tamil Nadu, India

Corresponding Author

***Dr. Amitava Mukherjee**

Senior Professor and Director

Centre for Nanobiotechnology

VIT, Vellore 632014, India

Email: amit.mookerjea@gmail.com, amitav@vit.ac.in

Tel.: +91 416 220 2620

SI.1 Nanocomposite beads preparation

Preparation of nanocomposite

Step 1: Formation of clay nanosheets (CNS)

The mixture of bentonite–deionized water (5 wt %) was stirred for 4h at 400 rpm. The large-sized sediments were removed from the mixture by centrifuging it at 1000 rpm for 1 min. The upper part was centrifuged at 10,000 rpm for 5 min to produce pure CNS. The purified CNS was combined with deionized water to produce a suspension of 7.6 wt% after performing 60% ultrasonication for 4 min.

Step 2: Synthesis of in-situ Fe/Cu CNS nanocomposite

In situ, CNS-based Fe-Cu nanoparticles were prepared using a liquid phase reduction technique. A suspension containing 2 wt% CNS was added to 0.1M $FeCl_3$ and 0.1M $CuCl_2$ mixture (ethanol: water - 4:1). Under the inert condition, the pomegranate rind extract (as a reducing agent) was added to the mixture drop by drop. Fe-Cu CNS nanocomposite formation is indicated by black precipitation seen over the CNS. The nanocomposites were filtered and vacuum-dried to produce pure Fe-Cu CNS.

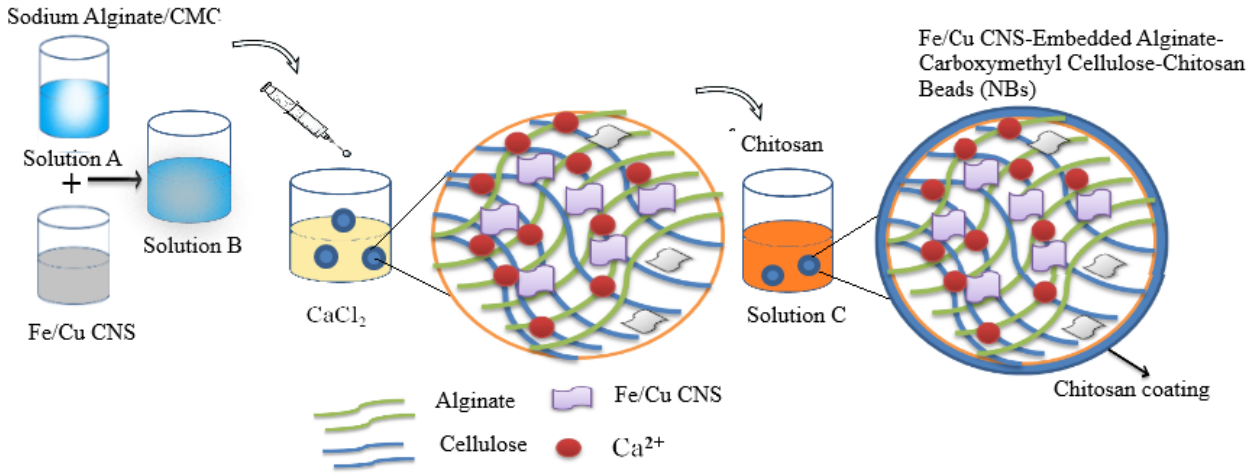

Fig.S1 Schematic representation of Fe/Cu CNS Embedded Alginate Carboxymethyl Cellulose-Chitosan Beads formation

S1.2 Point of Zero Charge (pH_{PZC}) measurement of NBs

The pH level at which an adsorbent surface has no net charge is known as pH_{PZC}. To determine pH_{PZC}, we prepared a series of flasks containing 50 mL of nitrogen-purged 0.1 M NaCl solutions. We adjusted the pH of the solutions to remain within the range of 2-10 using 0.1 M NaOH/0.1 M HCl. Then, we added 0.15 g of dried NC beads to each flask and stirred the mixture at room temperature for 24 hours at 150 rpm. Afterward, we filtered each solution and measured the pH again. The pH at which the curve intersects the initial bisector (pH_{final}=$pH_{initial}$) is known as pH_{PZC}.

SI. 3 NBs characterization study

Synthesized Fe/Cu CNS and NBs were confirmed by FTIR, XRD, and SEM-EDX in our earlier study. Furthermore, the swelling behaviour was analyzed by swelling measurements to check the stability of NBs during the treatment process. The NBs were uniform spheres with an average diameter of 2 mm. The structural morphology of the NBs is seen in the FESEM images (Fig. S2(a–b)). The NBs' surface was incredibly rough and dense, with many more wrinkles and inward holes at the μm level, which may have increased the number of adsorption sites available. The NB's increased surface area suggests that embedding chitosan over the NBs may improve the surface roughness of the NBs, which is directly related to the high SSA (specific surface area). Moreover, the surface area would be increased by the vacancies created during the surface amination by chitosan followed by freeze-drying of NBs. Besides, the EDX spectrum study for

the NBs and Fe/Cu Clay nanosheets nanocomposite (Fig.S2(c-d)) confirms the presence of Fe, Cu, Si, and Al. Also, for NB's EDX mapping, the high-intensity peak corresponding to C and O was noted. The NBs exhibit a low pore volume within the range of 0.20 nm and a higher SSA of 35 m^2/g, as determined by BET analysis. This assessment suggests that adding the nanocomposite enhances the pore volume and SSA of the control beads.

The FTIR spectrum of the Fe/Cu CNS and NBs (Fig.S3a) were gathered at a wavenumber scanning range from 4000 to 400 cm^{-1}. The spectral bands observed at 3440 cm^{-1} were assigned to the overlapping vibrations of the N-H and O-H groups, as illustrated in Fig. S3a. The existence of oxygen-containing functional groups on the surface of NBs, such as carboxyl and hydroxyl groups, has been found to have an important function in the NOR adsorption through hydrogen (H) bonding. The following can be used to assign the remaining peaks: a) peak observed at 1630 cm^{-1} corresponds to the characteristics of COO (asymmetric stretching), (b) Peak observed at approximately 1621 cm^{-1} corresponds to the stretching vibrations of the C-N and N-H functional groups associated with the amine groups, (c) Peak at 1425 cm^{-1} to the COO (symmetric stretching), and (d) The peaks at 612 and 526 cm^{-1} due to the Fe–O and Cu–O stretching e) The peak at 1019 cm^{-1} is assigned to the characteristic peak of clay nanosheets (Si–O stretching vibration).

XRD study was utilized to validate the crystal structure of the developed NBs. As shown in Fig.S3b, unique peaks related to various planes of NBs, namely (110), (210), (124), (110) and (144), were noted at 2θ values of 20.7◦, 26.5◦, 36.3◦, 44.8◦ and 54.7◦, respectively (JCPDS file card number 01-088-0891). The diffraction peaks of the NBs matched those of Fe/Cu CNS nanocomposite, offering strong proof of the effective loading of nanocomposite within the hydrogel beads.

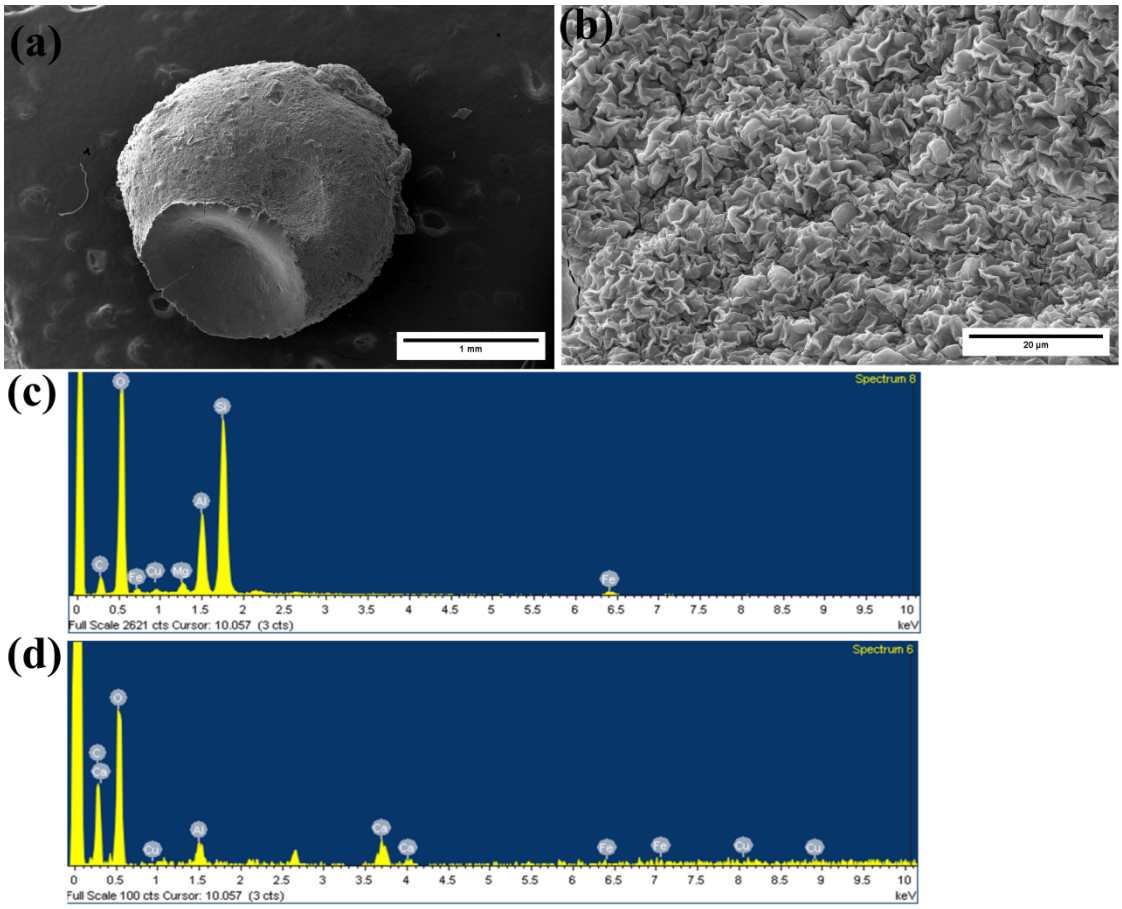

Fig.S2.(a-b) FE-SEM image of NBs (c-d) EDX spectrum of NBs and Fe-Cu CNS

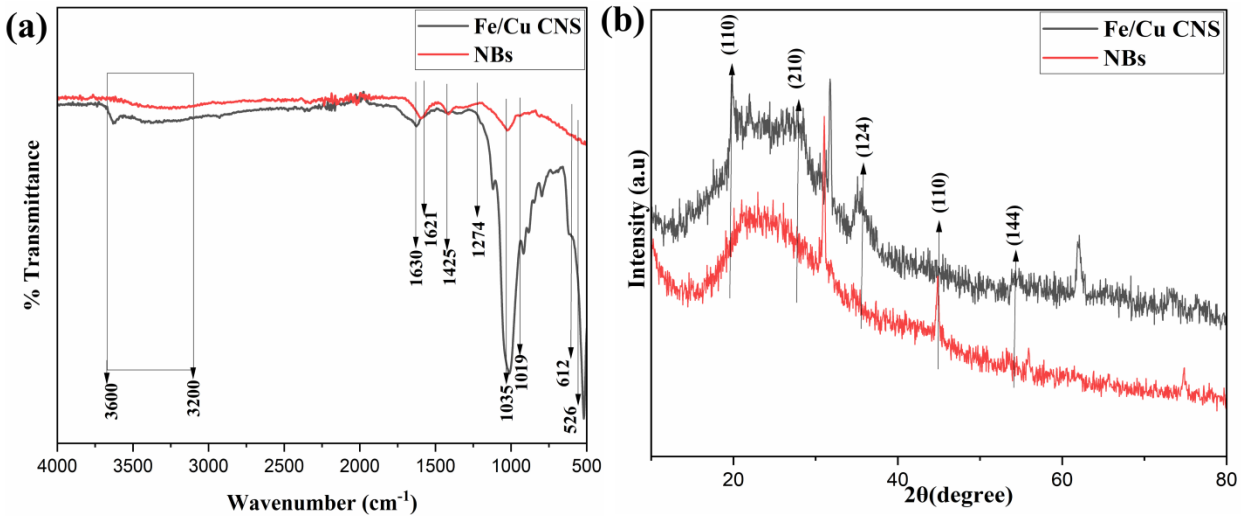

Fig.S3.(a) FTIR spectrum of NBs and Fe/Cu CNS (b) XRD of NBs and Fe/Cu CNS

SI.4 NOR absorption measurements by linear fitting

The compound NOR is distinguished by characteristic absorbance peaks at 276 nm, owing to its quinoline monocarboxylic structure. In order to track variations in absorbance during the NOR degradation process, UV-Vis spectra were recorded. A standard graph was plotted to determine the absorbance of various NOR concentrations (2.72-40 mg/L) at 276 nm. The correlation coefficient (R^2) was determined to be 0.97. Employing this calibration curve, the residual concentration of NOR following NBs treatment was determined.

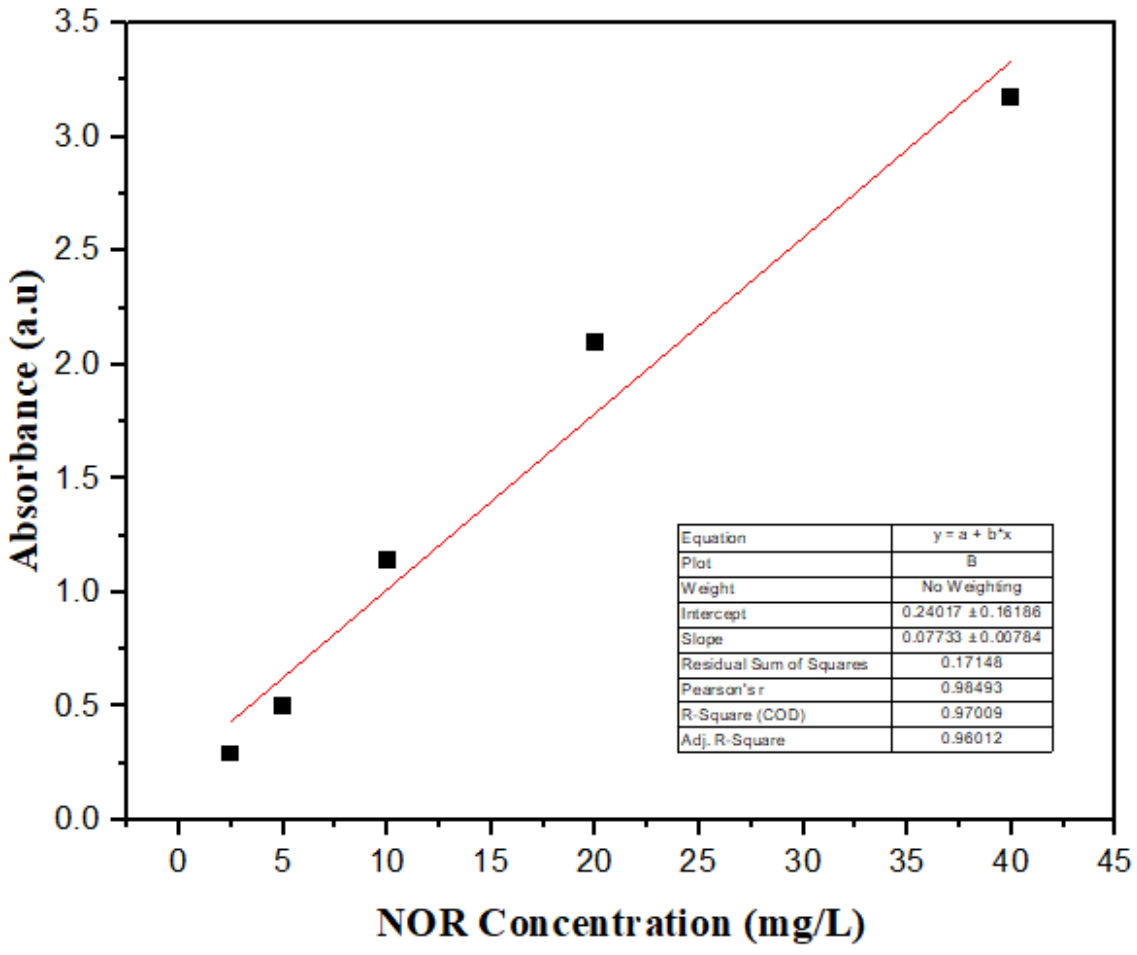

Fig.S4 Linear fit of NOR absorption spectrum (λ_{max} 276 nm)

SI.5 Effect of different parameters on NOR removal

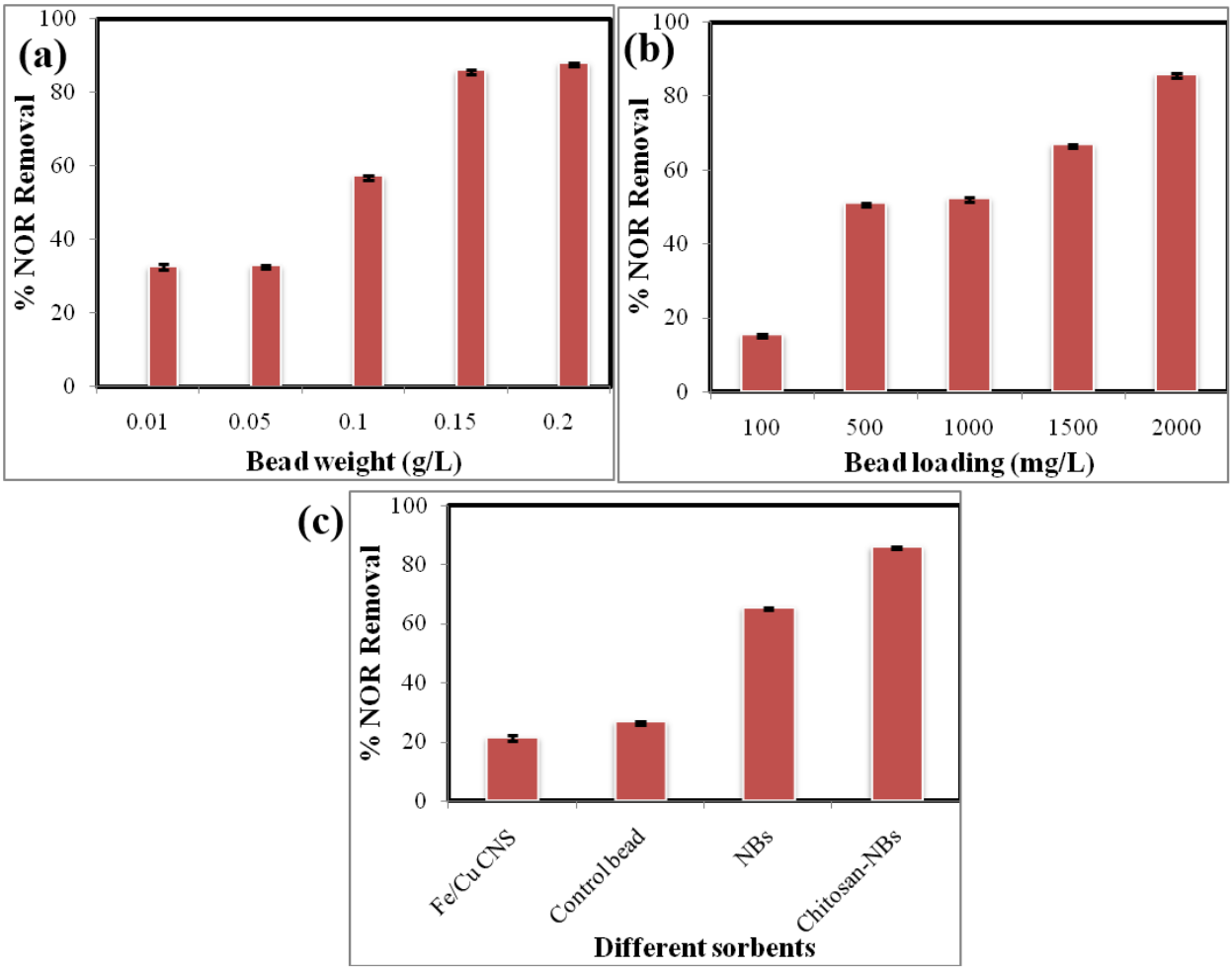

Fig.S5.Effect of (a) Bead weight (b) Bead loading and (c) Different sorbents on NOR removal

SI.6 Chromatogram analysis of treated NOR solution

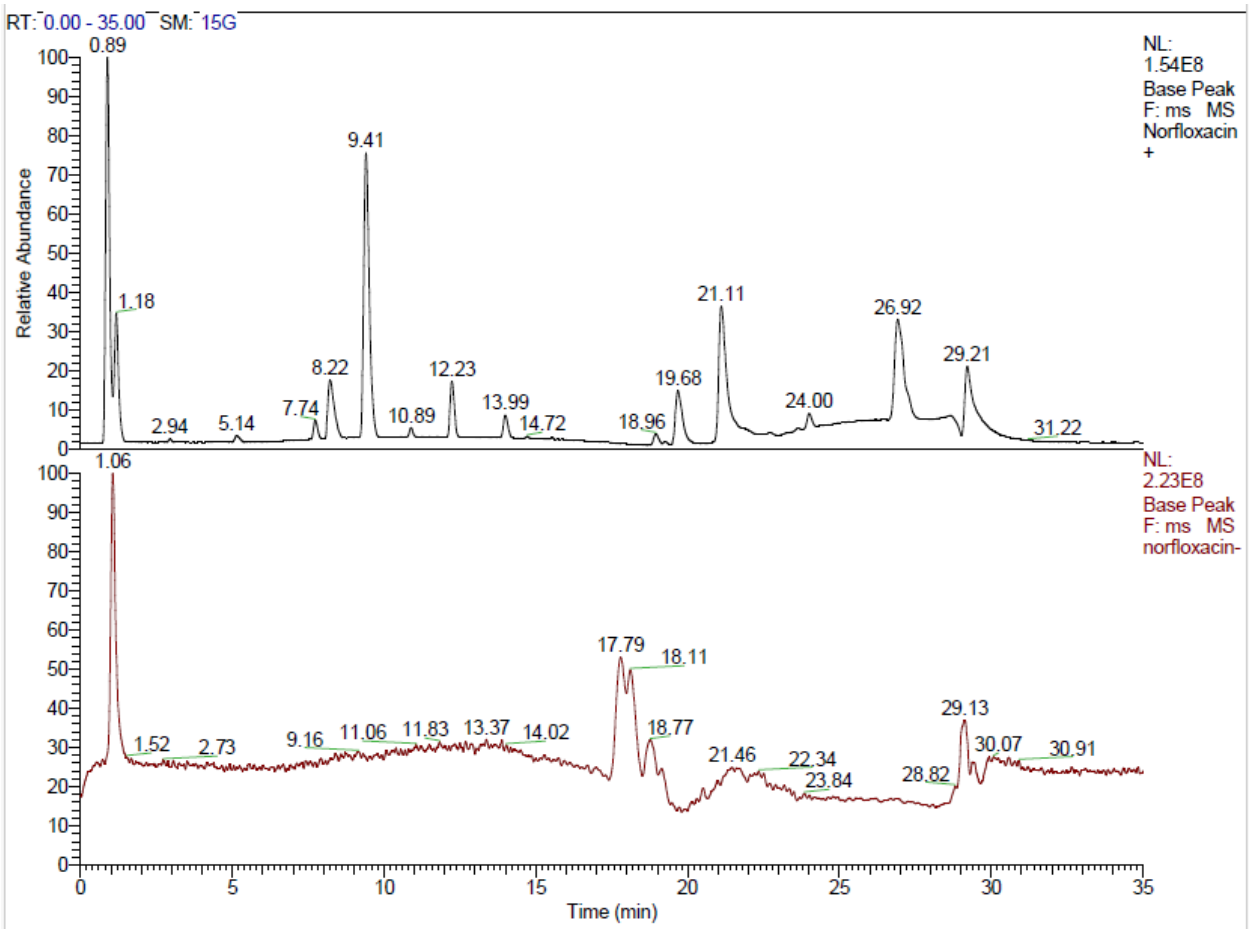

Fig.S6. Chromatogram of treated NOR solution

Table.S1. Synthetic effluent composition

Components	Concentration (mg/L)	Volume (500 mL)
Pharmaceuticals		
Paracetamol	10	5
Ibuprofen	10	5
Diclofenac	10	5
Tetracycline	10	5
Sulfamethoxazole	10	5
Erythromycin	10	5
Levofloxacin	10	5
Ciprofloxacin	10	5
Ampicillin	10	5
Sugars		
Sucarose	30	15
Glucose	30	15
Organic components		
Urea	10	5
Citric acid	10	5
Inorganic components		
Ammonium chloride	20	10
Sodium sulphate	10	5
Sodium carbonate	10	5

Sodium chloride	50	25